COMPUTATIONAL MODELING AND PREDICTING SPREAD OF ARBOREAL EPIDEMIC

ANKUSH RAI*, JAGADEESH KANNAN R

School of Computing Science & Engineering, VIT University, Chennai, Tamil Nadu, India. Email: ankushressci@gmail.com

ABSTRACT

Objective: This study presents a modeling solution for the arboreal epidemic like Huanglongbing. Usually, the spread of such plant disease is modeled based on the four parameters such as susceptibility, exposure, infectiousness, detection, and removed, but such a model is deprived by the time as a dimension to model such variations. Due to this, the time for which infection, exposure, detection, and removal time is censored form modeling studies of disease spread through heterogeneous plant species.

Methods: Here, we computationally modeled those key factors for Huanglongbing (HLB) spread and used image processing technique for aerial images for segmenting field which can be utilized for cut-off the prodigiously infected field regions

Results and Discussion: The research presented in this work characterize such heterogeneous transmission with the integration of temporal, spatial modeling of latent period of season and effects on the host, infection period, and dispersal parameters corresponding to the hostage. The outcome form this research will enable to control the arboreal epidemic.

Keywords: Arboreal epidemic modeling, Huanglongbing, Infection time, Hostage and season effects.

INTRODUCTION

Under the jeopardy of emerging epidemic, it is critical to gauge the key epidemiological factors to prognosticate the probability and degree of further spread, and adscititiously to quantify the viability of sundry methodologies for epidemic control [1,2]. Inference model is required in such heterogeneous scenarios of host population through which the epidemic is spreading to control the impacts of pathogen spread and disease control [3-5]. This information like denuded or irresistible status of the plant group are censored because numerous disease parameters are unobservable, and the information are erroneous for detection of disease and are censored in time [6,7]. The examples of spread used to gauge the dispersal and transmission parameters may likewise mirror the effects of ailment or vector control measures. Currently, the utilization of spatiotemporal dynamical models has been an expanding accentuation on to address the quandary of the transmission processes of epidemics [1,4]. For such dynamical models, the frequently assessed parameters might be fussed with generally constrained and skeptical information [5,6]. Non-monotonic logic inference, upheld by cutting-edge computational techniques, is especially tractable and is progressively the approach in this scenario [7-10]. Due to its advantage over other examination methods such models offer inferences from several interconnected obnubilated processes. Although there is withal a high need to incorporate the seasonal factors and the age of the host for epidemic dynamics [11-13]. These are a few extra challenges in assessing the key epidemiological parameters for a formerly obscure, elevating pathogen (Fig. 1).

METHODS

Here, to extract the features of uneven green coloring apart from its nature color in the fruits and leaves of the given sample of images we use Attribute based Level Adaptive Thresholding Algorithm (ABLATA) for feature extraction. Thus, based on weighted spatial localization of neighboring pixels the threshold value of the cluster is determined through sets of evolving Thresholding t using ABLATA [15,16]. Mathematically, an image is a two-dimensional (2D) function, f(x, y), where x and y are the coordinate values in spatial domain or plane; and the magnitude of f(x, y) is the intensity value of the pixel at (x, y).

If x, y and the magnitude of f(x, y) in an image are discrete quantities then the image is said to be digital image. Image may be represented as 2D matrices whose elements are intensities of pixels present in image. Almost all image processing related operations operate on these pixels either in spatial domain or in frequency domain or transform domain. The function f(x, y) can be expressed as

$$f(x,y)=\begin{bmatrix} f(0,0) & \cdots & f(0,N_y-1) \\ \vdots & \ddots & \vdots \\ f(N_x-1,0) & \cdots & f(N_x-1,N_y-1) \end{bmatrix}$$

(1)

Now, each digital image has certain finite number of elements characterized by some coordinate values and intensity value. The coordinate indicates the position of pixel in an image. In equation 1 the image elements $f(N_x-1, N_y-1)$ represent the maximum number of resolution starting from $f(0,0)$.

Suppose that f is the set of categorized pixels band and "P" is a uniformity predicate defined over groups of connected pixels. Segmentation is simply a partitioning of the set F into a set of connected subjects or regions $(P_1, P_2, \ldots P_n)$ such that $\bigcup_{i=1}^{n} P_i = F$ with $P_i \cap P_j = \varphi$ when $I \neq j$. The uniformity predicate $i = 1$ pixels represented as $P(P_j)$ is true for all regions P_i and $P(P_i \cup P_j)$ and is false when P_i is adjacent to P_j. The thresholding algorithm for binary images is applied as:

$$f_t := \sum_{i=0}^{m} r(\{g_i \le f_{block} < g_{i+1}\}$$

(2)

Where, r() is the mean value; g_i and g_{i+1} are the lower bound and upper bound, respectively, of the given thresholding pixel boundary condition.

The unnatural bias for partitioning is avoided by selecting small sets of points and different measure of dissociation. The problem with such criterion for thresholding is that it does not consider association with clusters. To circumvent this problem, the cost of thresholding

Fig. 1(a and b): Illustration of Huanglongbing epidemic and its feature extraction using the proposed method

at runtime as a function of the total pixel threshold to all those levels formed in the above step is determined and taken in account through the pixel association rule.

Thus, we have the generic equation normalization is defined as:

$$f_t\left(N_x, N_y\right) = \sum_{i=0}^{x} r\left(\frac{\text{cut }(N_x - 1, V)}{\text{assoc }(N_x - 1, N_y)} + \frac{\text{cut }(N_x, N_y)}{\text{assoc }(N_y, V)}\right) \quad (3)$$

Where, assoc $(N_x, N_y) = \Sigma_{X \in m, V \in n} W(u,v)$ is the total connection from pixels of set A to all set B. Using this definition of the disassociation between the groups, small isolated points are partitioned out and will no longer have distinct N values, since the cut value will almost be a large percentage of the total connections from the small set to all other pixels. If no other level changes are found then terminate the operation. The mechanism of segmented image is finally generated after extraction operation.

Thus, let us suppose that levels based dependencies between different colored parts can be expressed as p(A|B) where A is the sets of nodes estimated by ABLATA in previous steps during normalization and B is the voting element for A which express the feature description for the local sub-patches in form of a sets of nodes given by the training sets of a number of images on iteration basis [14]. Thus, the location of different parts is dependent, that is,

$$p(A|B) = \prod_{i=1}^{N} p(f_t|B) \quad (4)$$

However since, equation 4 creates a consolidated regions R_i from Levels L_i and Pixels p_i. Therefore, the entropy H of two positions can be mathematically defined as:

$$H(B) = \sum_{n=1}^{N} \frac{\sum_{i \in R_i} (A|B)}{\|B\|} \quad (5)$$

$$t_{f_t}\left(R_i, L_i\right) = \begin{cases} H(B), \text{ if } f_t\left(R_i, L_i\right) < S \\ H\left(A \bigcap B\right), \text{ if } f_t\left(R_i, L_i\right) > S \end{cases} \quad (6)$$

$$S = \frac{t_{f_t}}{\nabla t_{f_{t+1}}} \quad (7)$$

Where, S is the splitting function and $f(R_i, L_i)$ which is the function represented in equation 3 recursively with R_i and L_i as its hierarchical input parameters and t_{f_t} is the segmented region with integrated facial features.

Thereby, for all such functions comprising an image is a subset of V. This allows us to write a two-pixel image over the interval [0.1/2) to [1/2.1). On continuing this pattern, the traversal of the whole image can be summed into 2^j equal subintervals for V^j vector subspaces. Hence, the scaling functions of the wavelets can be written as:

$$\phi_j^i(x) = \phi\left(2^j - i\right) i = 0,1,2 \ldots 2^j - 1$$

$$\phi(x) := \begin{cases} 1 \text{ for } 0 \le x < 1 \\ 0 \text{ otherwise} \end{cases}$$

Thereby, the wavelet coefficients are given by:

$$\psi_j^i(x) = \psi\left(2^j x - i\right) i = 0,1,2 \ldots 2^j - 1$$

$$\psi(x) := \begin{cases} 1 \text{ for } 0 \le x < 1/2 \\ -1 \text{ for } 1/2 \le x < 1 \\ 0 \text{ otherwise} \end{cases}$$

Now for mapping the whole farm based on the severity of the infection as the color values ranges from red (worst) to green (un-infected) can be achieved based on the deviation of given sample images can be summed using standard deviation as function of covariance as represented below:

$$\delta_{ab}(t) \approx \frac{\text{cov }(G_a(t), G_b(t))}{\sigma_{y_a(t)} \cdot \sigma_{y_b(t)}}$$

Now, to form model for the epidemic spread let us suppose that e be the number of states of infection represented in the form of three colors where red represent infected, blue represent susceptible to get infected and green represent health state. Other parameters are: Passively immune can be presented by i_e, susceptible denoted as u_e and infectives be v_e. Similarly, the exposed period of infection in the latent period per specimen S is divided into two classes: Initial i_s and transfer function denoted as u_s. By considering the epidemic-secondary spread of infection availability of plants and density of immune plants, the equations that describe the spread of the epidemic signals can be written as:

$$\frac{di_e}{dt} = \mu_e + A - k_{+1}i_e - c(S)i_e u_s + \delta v_e$$

$$\frac{du_e}{dt} = c(S)i_e u_s - {}^3 u_e - k_{+1}u_e$$

$$\frac{dv_e}{dt} = k_{-1}\left(u_e\right) - k_{+1}v_e - \delta v_e$$

$$\frac{de}{dt} = \mu_e + A - k + 1e$$

$$\frac{di_s}{dt} = \mu_s - k_{-1}i_s - \beta_2 i_s u_e - \beta_3 i_s v_e$$

$$\frac{du_s}{dt} = -k_{-1}u_s + \beta_2 i_s u_e + \beta_3 i_s v_e$$

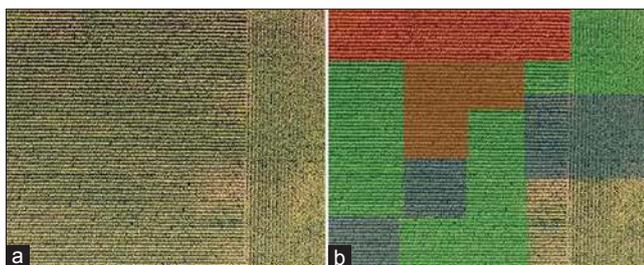$$\frac{dS}{dt} = \mu_s - k_{-1}e$$

Fig. 2: (a) Sample field for citrus plants for epidemic mapping (b) sample segmentation of the field using the row and column arrangement of each sample images from the field using the posteriors and subregions. The color of the region represents the severity of the infection as the color values ranges from red (worst) to green (un-infected). Orange represents the secondary spread of Huanglongbing
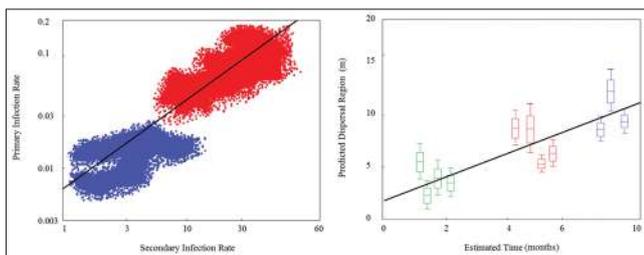

Fig. 3: Length scale of the dispersal kernel, α, by average age of subregion at estimated epidemic start time. The line in black is the linear model fitted to the mean length scale in terms of the mean age

Where, $e = i_e + u_e$ and $S = i_s + u_s$

In the system (1.1) μ_e, is priority index, A is the contact rate and k_{+1} is forward reaction rate constant. c is the total period of average immunity. γ is the recovery rate and δ is the parameter denotes the infection period such that the v_e will join the u_e class. μ_s is probability that the preceding delay threshold is violated and k_{-1} is its reverse latent period of signals. β_2 and β_3 are the interaction rates of operational number of plants with the initial and recovered classes, respectively ($\beta_2 > \beta_3$).

Since $i_e + u_e + v_e = e$ and $i_s + u_s = S$, the above system can be reduced to the form:

$$\frac{du_e}{dt} = c_0\left(e - u_e - v_e\right)u_s - (\gamma + k_{+1})u_e$$

$$\frac{dv_e}{dt} = \gamma\left(u_e\right) - (k_{+1} + \delta)v_e$$

$$\frac{de}{dt} = \mu_e + A - k_{+1}e$$

$$\frac{du_s}{dt} = -k_{-1}u_s + \beta_2(S - u_s)u_e + \beta_3(S - u_s)v_e$$

$$\frac{dS}{dt} = \mu_s - k_{-1}e$$

The region of prediction of the above system is:
$$T_1 = \left\{\left(u_e, v_e, e, u_s, S\right): 0 \le u_e + v_e \le N_1 \le \overline{e}, 0 \le u_s \le S \le \overline{S}\right\}$$

Here, the unique solution of the above equation exists in T for all positive values of dispersal time which are mathematically well posed (Fig. 2).

RESULTS AND CONCLUSION

When dealing with the emerging disease at rapid rate of transmission the requisite is to observe and model the key factors to initiate the control measures. Here, we computationally modeled those key factors for Huanglongbing (HLB) spread which can be utilized for cut-off the prodigiously infected field regions as shown in Fig. 3. Unlike other statistical technique, this provides an authentic time feasible solution by modeling anteriorly unidentified aspects of HLB, that is, its temporal model and sequence of infection spread. This investigation efficaciously showed how dispersal and transmission parameters for the case of HLB differed with host and temporal variation. We supplementally affirmed a direct relationship between primary and secondary infection zone represented in the form of orange in Fig. 2. This form a layout of getting an optional contamination to decide the cut-off regions for spread of disease and its control in a farm land.

Comprehension of different pathosystems of comparative intricacy and scale is represented in this study (Fig. 2). The output results exhibited the application of computational techniques to utilize infection spread through a spatially and transiently heterogeneous environment regardless of the secondary infection. The utilization of the parametric model to anticipate future results of HLB infection spread, and in additamet the adequacy of control, together with the consistency of results, for instance, concerning the impacts of time of host's infected period, all provide the quantifications to check the more periodic cycles and seasonal alterations to estimation of the prognostications from the model.

REFERENCES

1. Gibson GJ, Otten W, Filipe JA, Cook A, Marion G, Gilligan CA, *et al*. Bayesian estimation for percolation models of disease spread in plant populations. Stat Comput 2006;16(4):391-402.
2. Cook A, Marion G, Butler A, Gibson G. Bayesian inference for the spatio-temporal invasion of alien species. Bull Math Biol 2007;69(6):2005-25.
3. Kadoya T, Washitani I. Predicting the rate of range expansion of an invasive alien bumblebee (*Bombus terrestris*) using a stochastic spatio-temporal model. Biol Conserv 2010;143(5):1228-35.
4. Meentemeyer RK, Cunniffe NJ, Cook AR, Filipe JA, Hunter RD, Rizzo DM, *et al*. Epidemiological modeling of invasion in heterogeneous landscapes: Spread of sudden oak death in California (1990-2030). Ecosphere 2011;2(2):24.
5. Streftaris G, Gibson GJ. Bayesian analysis of experimental epidemics of foot-and-mouth disease. Proc Biol Sci 2004;271(1544):1111-7.
6. Cauchemez S, Boelle PY, Donnelly CA, Ferguson NM, Thomas G, Leung GM, *et al*. Real-time estimates in early detection of SARS. Emerg Infect Dis 2006;12(1):110-3.
7. Boys RJ, Giles PR. Bayesian inference for stochastic epidemic models with time-inhomogeneous removal rates. J Math Biol 2007;55(2):223-47.
8. Bettencourt LM, Ribeiro RM. Real time bayesian estimation of the epidemic potential of emerging infectious diseases. PLoS One 2008;3(5):e2185.
9. Deardon R, Brooks SP, Grenfell BT, Keeling MJ, Tildesley MJ, Savill NJ, *et al*. Inference for individual-level models of infectious diseases in large populations. Stat Sin 2010;20(1):239-61.
10. Gottwald TR. Current epidemiological understanding of *Citrus* huanglongbing. Annu Rev Phytopathol 2010;48:119-39.
11. Bové J. Huanglongbing: A destructive, newly-emerging, century-old disease of *Citrus*. Plant Pathol 2006;88(1):7-37.
12. Bassanezi RB, Montesino LH, Stuchi ES. Effects of huanglongbing on fruit quality of sweet orange cultivars in Brazil. Eur J Plant Pathol 2009;125(4):565-72.
13. Bassanezi RB, Montesino LH, Gasparoto MC, Filho AB, Amorim L. Yield loss caused by huanglongbing in different sweet orange cultivars in São Paulo, Brazil. Eur J Plant Pathol 2011;130(4):577-86.
14. Rai A, Ramanathan S. Distributed learning in networked controlled cyber physical system. Int J Pharm Technol 2016;8(3):18537-46.
15. Rai A. Attribute based level adaptive thresholding algorithm for object extraction. J Adv Robot 2015;1(2):64-8.
16. Rai A. Attribute based level adaptive thresholding algorithm (ABLATA) for image compression and transmission. J Math Comput Sci 2014;12:211-8.